THERMODINAMIC STUDY OF A HYBRID SOLID OXIDE FUEL CELL AND A GAS TURBINE CYCLE

Tássio Marques Rios, tassiomrios@hotmail.com
Elisângela Martins Leal, elisangelamleal@decat.em.ufop.br
Luis Antonio Bortolaia, luis.bortolaia@em.ufop.br
Department of Control and Automation Engineering, School of Mining, The Brazilian Federal University of Ouro Preto, Campus Morro do Cruzeiro S/N, Bauxita, Ouro Preto, Minas Gerais, Brazil. ZIP: 35.400-000

Julio Cesar Costa Campos, julio.campos@ufv.br
Department of Industrial and Mechanical Engineering, The Brazilian Federal University of Viçosa, Prof. Avenue Peter Henry Rolfs, Viçosa, MG, Brazil. ZIP: 36570-900.

Washington Orlando Irrazabal Bohorquez, washington.irrazabal@ufjf.edu.br
Department of Production and Mechanical Engineering, Faculty of Engineering, The Brazilian Federal University of Juiz de Fora, Juiz de Fora, MG, Brazil, ZIP: 36036-330.

Abstract. *In the last 10 years, research and development activities in fuel cell technology have been intensified within industry, research institutes and universities. As a result, fuel cells are now moving towards commercial readiness, or expecting a breakthrough within the next few years. The electricity production market benefits from combined or hybrid cycles because of their high efficiency. In this scenario, fuel cells are a good candidate combined to gas turbines. Systems studies indicate that fuel cell/turbine hybrid system could realize a 25 percent increase in efficiency for a comparably sized fuel cell. The synergy comprehended by fuel cell/turbine hybrid system derives primarily from the use of rejected thermal energy and combustion of residual fuel from a fuel cell to drive the gas turbine. High temperature fuel cells offer good opportunities for coupling with a gas turbine. This type of fuel cell allows the conversion of a wide range of fuels, including various hydrocarbon fuels. The relatively high operating temperature allows for highly efficient conversion to power, internal reforming, and high quality by-product heat for cogeneration or for use in a bottoming cycle. Fuel cell systems have demonstrated minimal air pollutant emissions and low greenhouse gas emissions. This paper presents a thermodynamic analysis of a direct internal reforming solid oxide fuel cell (DIR-SOFC) and a gas turbine (GT) system. Equilibrium calculations are performed to find the ranges of inlet steam/fuel ratio. After that, a hybrid system with a DIR-SOFC and a GT is evaluated using a computer simulation in the design point. The results showed that the fuel cell is the main energy producer system. Also, the high net efficiency (76%) is achieved by the hybrid cycle compared to fuel cell efficiency of about 48% and the gas turbine around 37%. Finally, it is shown that the computer simulation of the hybrid system may represent a quick and economic feasible way to investigate it.*

Keywords*: solid oxide fuel cell, gas turbine, hybrid system, energy analysis.*

1. NOMENCLATURE

A - Area [m^2 or cm^2]
C_p - Specific heat at constant pressure [kJ/kg.K]
C_v - Specific heat at constant volume [kJ/kg.K]
E - Operation cell voltage [V]
F_n - Faraday constant [96487.309 C/mol]
h - Specific enthalpy [kJ/kg]
i - Current [A]
i_L - Limiting current [A]
j - Current density [A/m^2]
j_0 - Exchange current density [A/m^2]
K - Reaction equilibrium constant [-]
LHV - Lower heating value [kJ/kg or kJ/kmol]
$\dot{m}$ - Mass flowrate [kg/s]
n_e - Number of electrons transferred per mole of fuel [mol e^-/mol]
P - Pressure [kPa or MPa]
p_i - Partial pressure of the component *i* [kPa]
$\dot{Q}$ - Heat transfer rate [kW]
$\bar{R}_g$ - Universal gas constant [8.315 kJ/kmol.K]
r_p - Pressure ratio [-]
R_t - Total resistance of the cell components [Ω]
rtc - Resistance to charge transfer [$\Omega.m^2$]
S - Entropy [kJ/K]
s - Specific entropy [kJ/kg.K]
T - Temperature [°C or K]
U_f - Fuel utilization [-]
W_{FC} - Electric energy density [J/m^2]
W - Work [kJ]
$\dot{W}$ - Power [kW]

GREEK LETTERS

ΔV_{act} - Activation Polarization [V]
ΔV_{conc} - Concentration polarization [V]
ΔV_{ohm} - Ohmic Polarization [V]
Δ_p - Pressure drop [kPa]
δ - Equivalent thickness of the diffusion layer [m]

η - Efficiency
η_{elec} - Electric energy efficiency
η_{GT} - Isentropic efficiency of the gas turbine [-]
η_{GTM} - Mechanical efficiency of the gas turbine [-]
η_{C} - Isentropic efficiency of the compressor [-]
η_{CM} - Mechanical efficiency of the compressor [-]
ρ_m - Resistivity [[Ω.m]
γ - Isentropic coefficient [-]

Subscripts
0 - Standard state (1 atm and 25ºC)
ac - Alternating current
an - Anode
cat - Cathode
∞ - Environment
C - Compressor
Comb - Combustor
dc - Direct current
FC - Fuel cell
Ger - Generator
GT - Gas Turbine
reg - Regenerator

2. INTRODUCTION

According to the International Energy Agency (IEA, 2015), the world consumed, in 2013, about 13.5 billion of tons of oil equivalent (toe), of which, 81.4% are from fossil fuels, responsible for CO_2 emissions of around 32.2 billion tons. According to the Energy Research Company (EPE, 2015), 37% of the World energy demand, or 4.8 billion of toe, were used in the electric energy generation, leading to 22,000 TWh generated. The economic development and the life standards sought by society are demands that require a reliable and trustworthy supply of energy (Barreto *et al.*, 2008).

The construction of nuclear, hydroelectric or thermal power plants have become impracticable, due to the inherent environmental impacts and associated risks. Such circumstances bring up the opportunity to evaluate new energy generation technologies (Neto, 2005). The constant need for clean and efficient energy generation systems have been taking technological development centers to search new, innovative ways to obtain maximum power and high efficiency with lower costs (Silveira *et al.*, 1999).

Such goals might be achieved mainly by improving existing systems and/or using clean energy (solar, wind) or renewable fuels (biomass, hydrogen), avoiding or even reducing the usage of fossil fuels which are the major contributors of carbon dioxide emissions (Bang-Møller *et al.*, 2013).

According to Carcasci *et al.* (2000), one of the ways to reduce the fossil fuel impact in the atmosphere is through more efficient energy generation systems, such as combined cycles. The biggest benefit of this type of combination is the better use of the fuel, in other words, more power can be harnessed from the same amount of fuel, thus increasing the system efficiency and lowering the release of pollutants *per* kilowatt-hour generated.

Recent studies related to the use of gas turbines and solid oxide fuel cells, known as hybrid systems, have been developed. Hybrid systems with the purpose of electric energy generation, as stated by Hauschild (2006), are systems composed by two or more energy production sources, operating together in order to attend a common consumer.

Granovskii *et al.* (2007) performed a research that included an exergy analysis of two gas turbine fuel cell hybrid systems to determine their efficiency and power generation capacity at different rates of oxygen transport through the cell electrolyte. Substantial works have been done to illustrate the efficiency of hybrid systems, which are able to reach of about 80% efficiency (LHV-based) when operating with natural gas as the fuel (McLarty *et al.*, 2014).

The thermal efficiency of an ordinary gas turbine plant has significant losses due to the high irreversibility inside the combustion chamber. A fuel cell gas turbine hybrid system represents an emerging technology to power generation, because of its higher efficiency in energy conversion, high synergy between equipment, low environmental impact and potential use of renewable energy sources as fuels (Magistri *et al.*, 2006).

This paper will technically analyze a hybrid system consisting of a direct internal reforming solid oxide fuel cell and a gas turbine in order to generate electric power with high efficiency. The thermodynamic simulation of the fuel cell has been made with EXCEL software, from where it was possible to obtain its operating parameters suitable to the hybrid cycle simulation. CYCLE-TEMPO software, from Delft University of Technology, was used to perform the thermodynamic simulation in the design point of the different equipment (fuel and air compressor, fuel cell, combustion chamber and gas turbine) of the system.

3. DESCRIPTION AND MATHEMATICAL MODELING OF THE HYBRID SYSTEM

Figure 1 shows the schematic diagram of the hybrid system in Cycle-Tempo software (Fig. 1a) and the temperature-entropy plot of the corresponding process (Fig. 1b). The first and second laws of thermodynamics are applied considering steady state of all equipment in the system and the working fluid is assumed to behave as an ideal gas. Figure 1a shows that (1) air enters the cycle through a compressor (C_1), where it is pressurized, leaving in the state (2). Compressed air is heated by the exhaust gases (6) from the gas turbine in the heat exchanger (E) that improves the total efficiency of the system. Thus, the heated compressed air (3) gets in the fuel cell (F) by the cathode side to participate in the electrochemical reaction. The fuel cell has an internal reforming system, in which a pressurized fuel is used (compressor C_2) along with steam. By the electrochemical conversion, direct current power (DC power) is produced by the fuel cell. However, due to the irreversibility of such process, especially ohmic resistances, heat is generated and the temperature of the products reaches state (4). The non-oxidized fraction of the fuel will be burnt in the combustion

chamber (G) of the gas turbine (T), located after the fuel cell. Therefore, the fuel cell products will get the desired temperature for the gas turbine entrance (5). Then, the combustion gas (5), which carries a certain amount of thermal energy, expands itself in the gas turbine in exchange for a heat loss, attaining state (6). The turbine supplies the power requirement of the compressor and provides additional power that will be summed with the power provided by the fuel cell. The turbine has an axle coupled to an electric generator that produces electric power in alternating current (AC). The exhaust gases from the turbine still have some thermal energy that is used by the heat exchanger to heat up the air that will be used by the cathode of the fuel cell, reaching, thus, state (7). The exhaust gas is released through the stack.

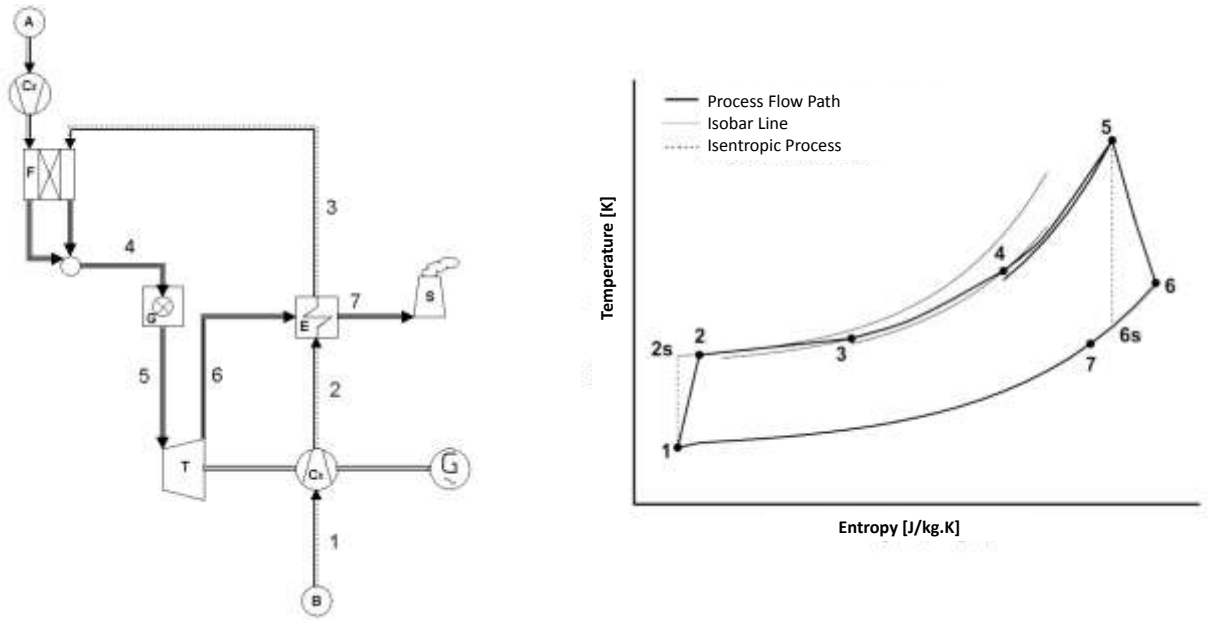

(a) Schematic of hybrid system. (b) Hybrid system temperature-entropy plot

Figure 1. Hybrid system (a) schematic and (b) temperature-entropy plot.

3.1 Solid Oxide Fuel Cell – SOFC

To a hydrogen fuel cell, with known pressures of the reactants and products (Chan *et al.*, 2001):

$$\mathrm{E} = \frac{\overline{\mathrm{R}}_\mathrm{g}\,\mathrm{T}}{2F_n}\ln \mathrm{K} - \frac{\overline{\mathrm{R}}_\mathrm{g}\,\mathrm{T}}{4F_n}\ln\left[\frac{p_{\mathrm{H_2O}}^2\,\mathrm{P}_0}{p_{\mathrm{H_2}}^2\,p_{\mathrm{O_2}}}\right] - \frac{\boldsymbol{S}_{\mathrm{ger,vc}}\,\mathrm{T}}{2F_n} \tag{1}$$

$$\frac{\boldsymbol{S}_{\mathrm{ger,vc}}\,\mathrm{T}}{2F_n} = \Delta\mathrm{V}_{\mathrm{ativ}} + \Delta\mathrm{V}_{\mathrm{ohm}} + \Delta\mathrm{V}_{\mathrm{conc}} \tag{2}$$

According to Chan *et al*. (2001), the first term on the right side of Eq. (1) shows the effect of temperature on the fuel cell potential, while the second term shows the effect of the pressure of the reactants and products on fuel cell potential. The effect of the irreversibility on the voltage drop is considered in the third term of the Eq. (1) and it can be expressed be the activation, ohmic, and concentration polarization (Eq. (2)).

Since the ionic flow of the electrolyte obeys the Ohm law, the losses by ohmic drop can be described by (Caires, 1996, Chan *et al.*, 2001):

$$\Delta\mathrm{V}_{\mathrm{ohm}} = i \times R_t \tag{3}$$

$$R_t = \frac{\rho_\mathrm{m}\,\delta}{\mathrm{A}} \tag{4}$$

$$\rho_\mathrm{m} = a\exp(b/\mathrm{T}) \tag{5}$$

Where: R_t is a total resistance of the fuel cell components, which can be calculated from its resistivity (ρ_m). The resistivity is a temperature function, where *a* and *b* are material specific constants. These constants are indicated in Tab. 1.

According to Caires (1996), chemical reactions, including electrochemical reactions, involve energy barriers that must be overcome by the reactants. This barrier is called activation energy. Activation polarization is produced because of the energy intensive activity of the making and breaking of chemical bonds at the cathode and anode. The amount of energy needed for the forming and destroying of these bonds comes from the fuel, and thus reduces the overall energy the cell can produce. The reduction is controlled by the reaction rate of the cell. If the reaction rate increases, the flow rate for fuel must also increase which increases the kinetic energy and thus lowers the energy required to break bonds. Increasing temperature, active area of the electrode and the utilization of the catalyst also lower the effect of activation polarization. To SOFC, the losses due to the activation polarization can be described as (Virkar *et al*. 2000, Chan *et al*. 2001):

$$\Delta V_{act} = \frac{2\bar{R}_g T}{n_e F_n} \sinh^{-1}\left(\frac{j}{j_0}\right) \tag{6}$$

Where j_0 is the exchange current density, that is a function of the fuel cell operating temperature and is related to the resistance of charge transfer (rtc) by:

$$j_0 = \frac{\bar{R}_g T}{n_e F_n \, rtc} \tag{7}$$

The resistance of charge transfer can be experimentally obtained or calculated from methods presented in the literature. Costamagna *et al.* (1998) shows the resistance calculation from the sum of two parts: the ionic conductor resistance and the electronic conductor resistance. On the other hand, Virkar *et al.* (2000) and Tanner *et al.* (1997) show the resistance calculation from physical and electrochemical properties of the material that compose the electrode of the SOFC.

According to Zhu *et al.* (2015), the concentration polarization becomes significant when big amounts of current are extracted from the fuel cell. The partial pressures of the gases in the reaction sites, which corresponds to their volume concentration, are smaller than in the bulk of the gas flow, when a big amount of current is extracted. This occurs in cases when the reactant transportation to the active sites is done in an inferior rate than the two subsequent stages, that is, its dissolution in the electrolyte or consumption in the ongoing reaction. This concentration gradient might originate a severe polarization and, then, a limiting current (i_L). In practice, the electrodes must have a wide interfacial area and be porous to ensure a reactants easy and continuous access. The concentration polarization can be calculated from (EG&G Services Parsons, Inc., 2000):

$$\Delta V_{conc} = \frac{R_g T}{n_e F_n} \ln\left(1 - \frac{i}{i_L}\right) \tag{8}$$

Once all losses by polarization are calculated, the fuel cell voltage can be determined by deducting the losses by polarization from the Nernst potential. The electric energy density produced by the fuel cell can be calculated as (Chan *et al.*, 2002):

$$W_{FC} = E.\, j \tag{9}$$

3.2. Gas turbine in a hybrid system

The concept of using a gas turbine in a SOFC integrated system have been well known for years. A research in the literature indicates that the concept was first analyzed by Ide *et al*. (1989), who compared three different hybrid systems in terms of net efficiency, energy generation, and energy recovery.

All the gas turbine modeling is based on Fig. 1b. The isentropic efficiency of the compressor is defined as (Van Wylen *et al*., 2003):

$$\eta_C = \frac{W_{Cs}}{W_C} = \frac{h_{2,s} - h_1}{h_2 - h_1} \tag{10}$$

Where the ideal temperature of the working fluid at the compressor outlet can be determined using the following equation **(**Van Wylen *et al*., 2003):

$$\frac{T_{2s}}{T_1} = \left(\frac{P_2}{P_1}\right)^{(\gamma-1)/\gamma} \tag{11}$$

γ is the ratio between specific heats at constant pressure (C_p) and constant volume (C_v). Applying the energy balance in the system, the work required for the compressor is (Van Wylen *et al*., 2003):

$$\dot{W}_C = \dot{m}_1(h_2 - h_1) \tag{12}$$

Besides, the equation for the entropy equilibrium for the compressor can be written as follow (Van Wylen *et al*., 2003):

$$\dot{W}_C = \dot{m}_1 S_1 - \dot{m}_2 S_2 + S_C = 0 \tag{13}$$

Thereby, the entropy generation rate during the process of compression can be obtained from the following equation (Van Wylen *et al*., 2003):

$$S_C = \dot{m}_1(S_2 - S_1) \tag{14}$$

The first law of thermodynamics for the combustion chamber can be expressed as (Cohen *et al.*, 1996):

$$(\dot{m}_{air,FC} + \dot{m}_{fuel,FC} U_f) + \dot{m}_{fuel,FC}(1 - U_f) = \dot{m}_4 = \dot{m}_5 \tag{15}$$

$$\dot{Q}_{comb} = \dot{m}_{fuel,FC}(1 - U_f) LHV \tag{16}$$

$$\dot{Q}_{Loss} = \dot{m}_{fuel,FC}(1 - U_f)(1 - \eta_{Comb}) LHV \tag{17}$$

η_{Comb} represents the efficiency of the combustor. The equation of entropy balance for the combustor can be written as (Cohen *et al.*, 1996):

$$m_4 s_4 + \frac{\dot{Q}_{Comb}}{T_{Comb}} + S_{Comb} - m_5 s_5 - \frac{\dot{Q}_{Loss}}{T_\infty} = 0 \tag{18}$$

Thus, the entropy generation rate inside the combustion chamber is (Cohen *et al.*, 1996):

$$S_{Comb} = m_5 s_5 - m_4 s_4 + \frac{\dot{Q}_{Loss}}{T_\infty} - \frac{\dot{Q}_{Comb}}{T_{Comb}} = 0 \tag{19}$$

Where T_{Comb} refers to the adiabatic flame temperature of, in which the heat is transferred to the working fluid.

As previously said, the work demanded by the compressor is provided by the gas turbine. Therefore, the net work of the gas turbine is given by (Van Wylen *et al*., 2003):

$$\mathrm{W_{net,GT}} = \mathrm{W_{GT}} - \mathrm{W_C} \tag{20}$$

Knowing the turbine inlet temperature, the turbine outlet temperature can be calculated through the definition of isentropic efficiency of the turbine (Van Wylen *et al*., 2003):

$$\eta_{\mathrm{GT}} = \frac{\mathrm{W_{GT}}}{\mathrm{W_{GTs}}} = \frac{\mathrm{h_5 - h_6}}{\mathrm{h_5 - h_{6,s}}} \tag{21}$$

Equation (22) give the gas turbine exit pressure as (Van Wylen *et al*., 2003):

$$\mathrm{P_6} = \mathrm{P_5}\left(\frac{\mathrm{T_{6,s}}}{\mathrm{T_5}}\right)^{\gamma/(\gamma-1)} \tag{22}$$

The equation of entropy balance for the turbine can be obtained with (Van Wylen *et al*., 2003):

$$\dot{m}_5 s_5 - \dot{m}_6 s_6 + S_{GT} = 0 \tag{23}$$

From the mass conversion, $\dot{m}_5 s_5 = \dot{m}_6 s_6$. The entropy generation rate during the expansion process is (Van Wylen *et al*., 2003):

$$S_{GT} = \dot{m}_5 (s_6 - s_5) \tag{24}$$

The regenerator efficiency is described as (Van Wylen *et al*., 2003):

$$\eta_{\mathrm{reg}} = \frac{\mathrm{T_3 - T_2}}{\mathrm{T_6 - T_7}} \tag{25}$$

Using the following energy balance equation, one may find the outlet temperature of the cycle (Van Wylen *et al*., 2003):

$$\dot{m}_2 (h_3 - h_2) = \dot{m}_6 (h_6 - h_7) \tag{26}$$

Besides, the entropy balance equation for the regenerator can expressed as (Van Wylen *et al*., 2003):

$$\dot{m}_2 s_2 + \dot{m}_6 s_6 + \dot{m}_3 s_3 + \dot{m}_7 s_7 + S_c = 0 \tag{27}$$

From the mass conservation ($\dot{m}_2 = \dot{m}_3$ and $\dot{m}_6 = \dot{m}_7$). Thus, the entropy generation rate inside the heat exchanger can be achieved with (Van Wylen *et al*., 2003):

$$S_{\mathrm{reg}} = \dot{m}_2 (s_3 - s_2) - \dot{m}_6 (s_6 - s_7) \tag{28}$$

3.3. Equations for general balance for hybrid cycle

The SOFC gas turbine hybrid system shown in Fig. 1 can be analyzed as a single control volume. The mass balance of the hybrid system can be described as:

$$\dot{m}_1 + \dot{m}_{fuel,FC} - \dot{m}_7 = 0 \tag{29}$$

$$\dot{m}_1 = \dot{m}_2 = \dot{m}_3 \tag{30}$$

$$\dot{m}_5 = \dot{m}_6 = \dot{m}_7 \tag{31}$$

On the other hand, the energy balance (first law) of the system is given by:

$$\dot{m}_1 h_1 + \dot{m}_{fuel,FC} \times U_f \times \mathrm{LHV_{CH_4}} + \dot{Q}_{Comb} - \dot{m}_7 h_7 - \dot{Q}_{Loss} - \dot{W}_{FC,dc} - \dot{W}_{net,GT} = 0 \tag{32}$$

$\dot{Q}_{Comb}$ and $\dot{Q}_{Loss}$ have been previously defined by the Eq. (16) and (17), respectively. The total thermal yield of the plant GT-SOFC is defined by the ratio between the net work and the total income power of the system.

$$\eta_{\text{tot}} = \frac{\dot{W}_{\text{net}}}{\dot{Q}_{\text{tot}}} \tag{33}$$

$$\dot{W}_{net} = \dot{W}_{FC,ac} + \dot{W}_{Ger} \tag{34}$$

$$\dot{W}_{FC,ac} = \eta_{\text{inverter}} \dot{W}_{FC,dc} \tag{35}$$

$$\dot{W}_{\text{Ger}} = \eta_{\text{Ger}} \dot{W}_{\text{net,GT}} \tag{36}$$

$$\dot{Q}_{\text{tot}} = \dot{m}_{\text{fuel,FC}} \times U_f \times \text{LHV}_{\text{CH}_4} + \dot{Q}_{\text{Comb}} \tag{37}$$

In which η_{inverter} and η_{Ger} are the inverter (DC to AC) and the generator efficiency, respectively.
Finally, the entropy generation rate within the system is the summation of entropy generated in all plant components.

$$S_{\text{cycle}} = \sum_i S_i \tag{38}$$

Where *i* is for compressor, regenerator, SOFC, combustor and gas turbine. The sum of Eqs. (2), (14), (19), (24) and (28) yields:

$$S_{\text{cycle}} = \dot{m}_7 s_7 - \dot{m}_1 s_1 - \frac{\dot{Q}_{Comb}}{T_{Comb}} + \frac{\dot{Q}_{Loss}}{T_7} \tag{39}$$

3.4. Hybrid system simulation

Table 1 indicates the physical properties of the fuel cell chosen to the present study, according to data given by the literature (Hirschenhofer *et al.*, 1994; Chan *et al.*, 2003; Virkar *et al.*, 2000; Zhu *et al.*, 2015).

Table 1 – Characteristics of the SOFC components (Hirschenhofer *et al.*, 1994; Chan *et al.*, 2003; Virkar *et al.*, 2000).

	Anode	**Electrolyte**	**Cathode**	**Interconnector**
Material	*Ni/YSZ*	*YSZ*	*LSM/YSZ*	*Mg/LaCrO$_3$*
Ohmic Resistance Constant	a = 0,0000298 b = -1392	a = 0,0000294 b = 10350	a = 0,0000811 b = 600	a = 0,001256 b = 4690
Thickness	$1{,}5\times10^{-4}$ m	$4{,}0\times10^{-5}$ m	$2{,}0\times10^{-3}$ m	$1{,}5\times10^{-4}$ m

Table 1 information will be used in the calculation of the SOFC polarization losses. Some general hypothesis have been made: the system operates in steady state; the processes are adiabatic; both the fuel cell and the regenerator operate in cross flow; the electric generator has an efficiency of 97%. Table 2 shows the system components, their identifications and the entry parameters of each equipment.

Table 2 – Equipment entry parameters.

Reference	**Name**	**Parameters**		
A	Fuel source	CH_4: 30% and H_2O:70%. Pressure = 1.013 bar.		
B	Air source	N_2: 77.29%, O_2: 20.75%, H_2O: 1.01%, CO_2: 0.03% and Ar: 0.92% Pressure = 1.013 bar and Temperature = 20°C.		
T	Turbine	η_{GT} = 0.85	η_{GTM}= 0.99	
G	Combustor	Δ_p = 0.3bar		
S	Stack	P_{in} = 1.013bar		
F	Solid Oxide Fuel Cell	$\Delta_{p,an}$ = 0.2bar $\Delta_{p,cat}$ = 0.2bar $T_{in,an}$ = 800°C	T_{FC} = 1000°C U_f = 0.85 η_{inv} = 0.97	R_{FC} = 5×10^{-5}ohm.m^2 j = 2500 A/m^2 A_{FC} = 800m^2
C$_1$	Turbine compressor	η_{C1} = 0.80	η_{CM1} = 0.98	r_p = 8
E	Regenerator	$\Delta_{p.hot}$ = 0.1 bar	$\Delta_{p.cold}$ = 0.1bar	$T_{out.cold}$ = 800°C
C$_2$	Fuel compressor	η_{C2} = 0.70	η_{CM2} = 0.98	r_p = 8

The Microsoft EXCEL software was used to perform the fuel cell thermodynamics simulation, and generate the specific plot of fuel cell energy density in function of the fuel cell current density. The thermodynamic simulation of the hybrid system was made through the CYCLE-TEMPO software, from Delft University of Technology.

4. RESULTS AND DISCUSSION

Figure 2 shows the results for the SOFC ohmic polarization for an anode (a), cathode (b) and electrolyte (c) supported fuel cell as a function of current density for temperatures ranging from 800°C to 1100°C.

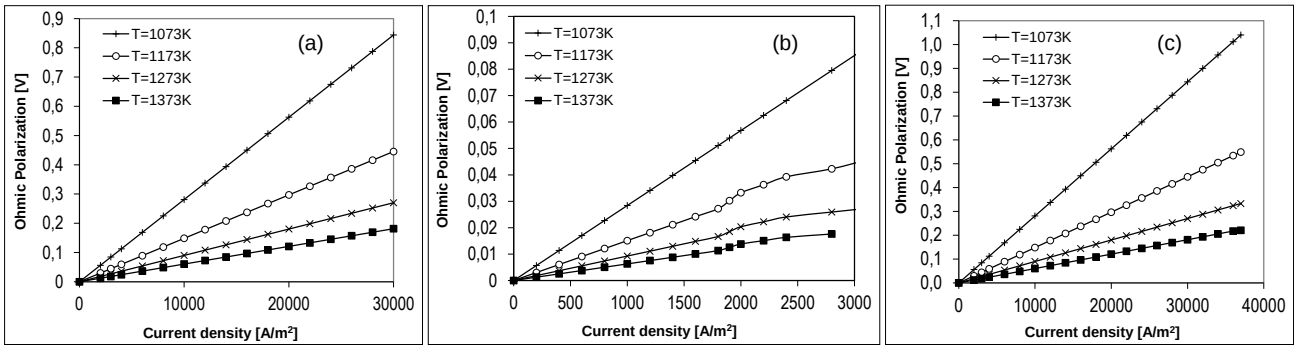

Figure 2. Results for ohmic polarization as a function of current density for the (a) anode supported, (b) cathode supported and (c) electrolyte supported SOFC (800°C ≤ T ≤ 1100°C).

It is observed that the ohmic polarization decreases with increasing temperature. Also, the component that most contributes to ohmic losses is the electrolyte, a fact that has become unviable the fuel cell development supported on it, according to Mahato (2015).

Figure 3a shows the exchange current density as a function of SOFC temperature. With these results, it was possible to calculate the activation polarization as a function of current density for temperatures ranging from 800°C to 1100°C. The results of activation polarization are shown in Fig. 3b.

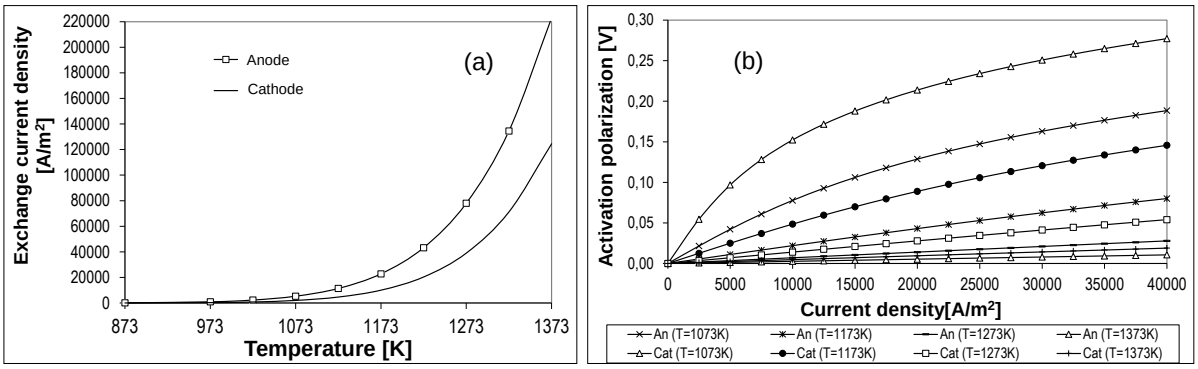

Figure 3. Results of the exchange current density as a function of temperature (a) and activation polarization for the anode and cathode-supported fuel cell (b) as a function of current density (800°C ≤ T ≤ 1100°C).

It is observed from Fig. 3 that the higher the temperature is, the lower the activation polarization is. Note also that the activation polarization is more significant at the cathode than at the anode.

Figure 4 displays the results of concentration polarization as a function of current density for temperatures ranging from 800°C to 1100°C, to fuel cells supported on the anode (Fig. 4a), cathode (Fig. 4b), and electrolyte (Fig. 4c). The results were constructed assuming a fuel containing 97% by volume of hydrogen and 3% by volume of water and air as the oxidant, a porosity of 30%, and a tortuosity factor of 6 (Chan *et al.*, 2002).

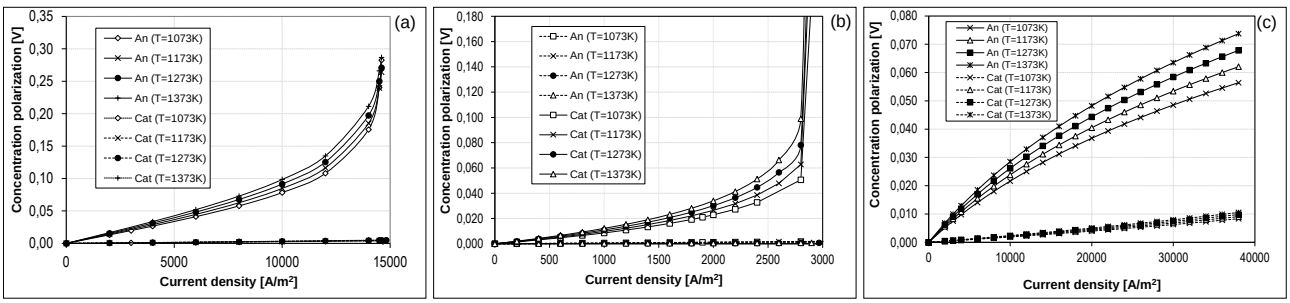

Figure 4 – Results of concentration polarization *versus* current density for the anode (a), cathode (b) and electrolyte (c) supported SOFC (800°C ≤ T ≤ 1100°C).

In the anode-supported fuel cell, it is noted that the anode polarization is more significant than the cathode and there is a limit to the anode current, which value decreases with increasing temperature. In this case, a mixture hydrogen/steam were used as the fuel. If used was natural gas as fuel, the value of limiting current density would decrease significantly (Chan *et al.*, 2002). Also, it is observed in cathode-supported fuel cell, the cathode polarization is more significant than in the anode and there is a limit to the cathode current, which value decreases with increasing temperature. If pure oxygen were used as the oxidant, this value would increase significantly (Chan *et al*., 2002). The concentration polarization in the electrolyte-supported fuel cell is smaller than other types, which does not influence significantly in the performance of the device.

Figure 5 illustrates the results of voltage *versus* current density for the anode (Fig. 5a), cathode (Fig. 5b) and electrolyte-supported (Fig. 5c) solid oxide fuel cell. It is observed that the fuel cell output voltage increases with increasing temperature in any of the types of fuel cell configuration. In addition, the increase in the fuel cell current density causes the decrease of the output voltage, which can permanently damage the components. In practice, it is recommended to work at the design point voltage of the fuel cell.

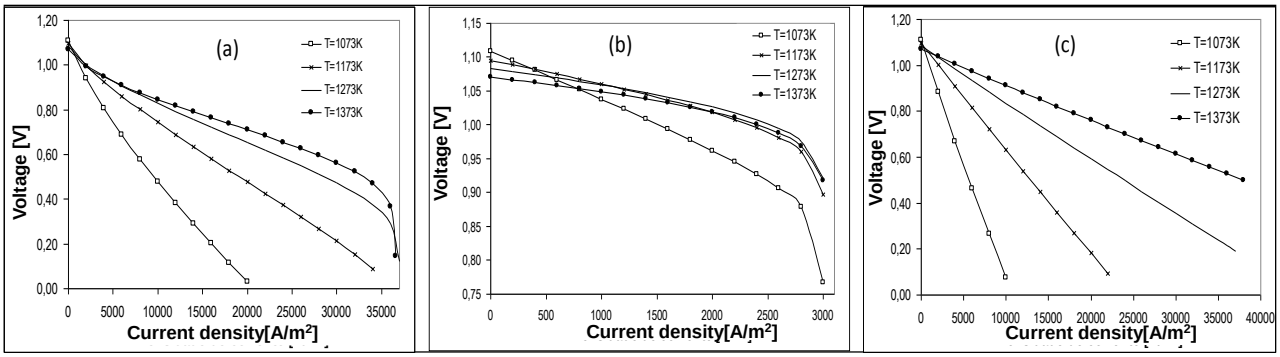

Figure 5 – Results of voltage *versus* current density for the anode (a), cathode (b) and electrolyte (c) supported SOFC (800°C ≤ T ≤ 1100°C).

The performance results of the fuel cell *versus* temperature are shown in Fig. 6, for the fuel cell supported at the anode (Fig. 6a), cathode (Fig. 6b) and electrolyte (Fig. 6c).

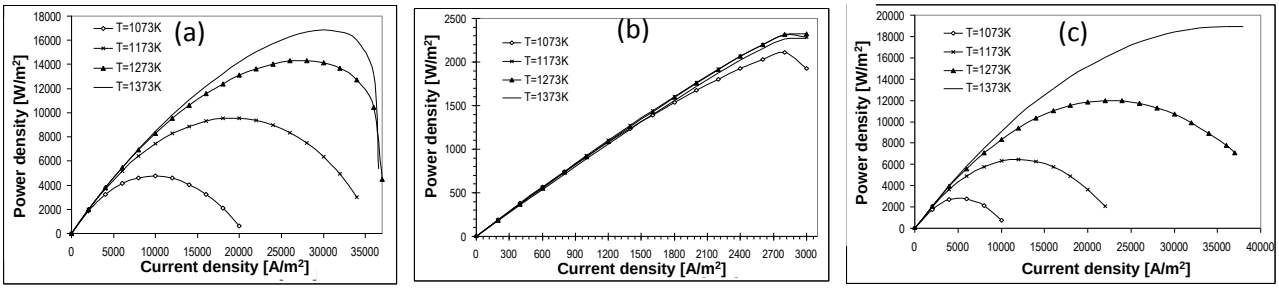

Figure 6 – Results of power density versus current density for anode (a), cathode (b) and electrolyte (c) SOFC (800°C ≤ T ≤ 1100°C).

It is observed through Fig. 6(a), (b) and (c) that the cathode-supported SOFC operates at lower current density than the others do because it has a limit current density lower than that of the other fuel cell configurations. Note that the higher the operating fuel cell temperature, the higher the peak power density. The operating temperature is limited by the physical integrity of the fuel cell components. The fuel cell chosen to the hybrid system is a tubular cathode-supported SOFC with internal reforming. Manufacturers such as Siemens Westinghouse use this setting, mainly due to its ease of construction related to sealing aspects (Mahato, 2015).

Although fuel cells can operate at any current density, researchers and suppliers recommend the use in a current density lower than where it reaches its power density peak. Therefore, the simulation of a hybrid system considers a fuel cell working at 2500 A/m^2. In addition, a 1 MW gas turbine was chosen for the study. The results of the hybrid system simulation are shown in Tab. 3.

Table 3. Results of the SOFC-GT hybrid system at the design point.

SOFC	Turbine	Compressor	Mass flowrate	Hybrid Cycle
j = 2500 A/m^2	$\dot{W}_{GT} = 975.33\,kW$	$\dot{W}_{C_1} = -463.06\,kW$	$\dot{m}_{comb} = 0.177$ kg/s	η_{NET} = 76.39%
E = 0.8124 V				
W = 2030 W/m^2		$\dot{W}_{C_2} = -204.82\,kW$	$\dot{m}_{air} = 1.517$ kg/s	$\dot{W}_{tot,NET} = 1868.2\,kW$
$\dot{W}_{FC} = 1576.12\,kW$				

It becomes clear that, in the design point**,** the fuel cell is the main energy generator, while the turbine is the second. It is also notable the high liquid efficiency (76.39%) reached by the hybrid cycle. While operating separately, the electric energy generation efficiency of the same cell is around 48%, and the turbine, 37%.

5. ACKNOWLEDGEMENTS

The authors acknowledge FAPEMIG (Foundation for the Research Support of Minas Gerais State – Process number TEC APQ 02156-14), the Federal University of Ouro Preto (UFOP) and Gorceix Foundantion for the financial support to this work. Also, thanks for those who helped in the execution of this research project.

6. REFERENCES

BANG-MØLLER, C. ROKNI, M. ELMEGAARD, B. AHRENFELDT, J. HENRIKSEN, U. B.. Decentralized combined heat and power production by two-stage biomass gasification and solid oxide fuel cells. Energy, v. 58, p. 527–537, 2013.

BARRETO, E. J. F.; PINHO, J. T; BARBOSA, C. F. O.; PEREIRA, E. F. S.; SOUZA, H. M. S.; BLASQUES, L. C. M.; GALHARDO, M. A. B.; MACÊDO, W. N. Sistemas híbridos – Soluções energéticas para a Amazônia. Programa Luz para Todos, 1ª edição, Brasília, Ministério de Minas e Energia, 2008.

CAIRES, M. I. Desenvolvimento e caracterização de matrizes a base de SiC, NbC e ZrSiO4 para células a combustível de ácido fosfórico. São Carlos, 1996. 103p. Dissertação (Mestrado em Ciências e Engenharia de Materiais) - Instituto de física e química de São Carlos, Universidade de São Paulo.

CARCASCI, C.; FACCHINI, B. Comparison Between Two Gas Turbine Solutions to Increase Combined Power Plant Efficiency; Energy Conversion & Management; vol 41; pp. 757-773, 2000.

CHAN SH, HO HK, TIAN Y. Multi-level modeling of SOFC–gas turbine hybrid system. Int J Hydrogen Energy, v. 28, p.889–900, 2003.

CHAN, S. H., KHOR, K.A. and XIA, Z.T. A complete polarization model of a solid oxide fuel cell and its sensitivity to the change of cell component thickness. Journal of Power Sources. Vol.93, pp. 130 - 140, 2001.

CHAN, S. H., LOW, C.F. and DING, O.L. Energy and exergy analysis of simple solid-oxide fuel-cell power systems. Journal of Power Sources. Vol.103, Issue 2, pp. 188 - 200, 2002.

COHEN, H.; ROGERS, G. F. C. e SARAVANAMUTTOO, H. I. H. Gas Turbine Theory. 4ª ed. Harlow: Longman, 1996.

COSTAMAGNA, P., COSTA, P., ANTONUCCI, V. Micro-modelling of solid oxide fuel cell electrodes. Electrochimica Acta. Vol. 43, n. 3 - 4, pp. 375 - 394, 1998.

EG&G SERVICES PARSONS, INC. Fuel Cell Handbook (Fifth Edition). West Virginia: National Energy Technology Laboratory, U.S. Department of Energy, contract no. DE-AM26-99FT40575, 2000.

EPE - EMPRESA DE PESQUISA ENERGÉTICA. Balanço Energético Nacional 2015. Ministério de Minas e Energia - MME. Available at: <https://ben.epe.gov.br/downloads/Relatorio_Final_BEN_2015.pdf>. Accessed in 06/03/2016.

GRANOVSKII, M. DINCER I. ROSEN, M. A. Performance comparison of two combined SOFC-gas turbine systems," Journal of Power Sources, vol. 165, pp. 307-314, 2007.

HAUSCHILD, L. Avaliação de Estratégias de Operação de Sistemas Híbridos Fotovoltaico-Eólico-Diesel. São Paulo: dissertação de mestrado em energia – USP (Programa Interunidades de Pós-Graduação em Energia), p.117, 2006.

HIRSCHENHOFER, J. H., STAUFFER, D. B. and ENGLEMAN, R. R. Fuel cells: a handbook (3rd revision). Philadelphia: Gilbert and Commonwealth, Inc., U.S. Department of Energy, contract no. DE-AC01-88FE61684, pp. 2-1 – 2-8, 1994.

IDE H, YOSHIDA T, UEDA H, HORIUCHI N. Natural gas reformed fuel cell power generation systems-a comparison of three system efficiencies. In Proceedings of the 24th Intersociety Energy Conversion Engineering Conference, vol. 3 1517–1522, Washington, DC, 1989.

IEA - International Energy Agency. Key World Energy Statistics. Available at <https://www.iea.org/publications/freepublications/publication/KeyWorld_Statistics_2015.pdf>. Accessed in 06/03/2016.

LIM TH, SONG RH, SHIN DR. Operating characteristics of a 5 kW class anode-supported planar SOFC stack for a fuel cell gas turbine hybrid system. Int J Hydrogen Energy, v. 33, n. 3, p. 76–83, 2008.

MAGISTRI L, TRAVERSO A, MASSARDO AF, SHAH RK. Heat exchangers for fuel cell and hybrid system applications. Jornal Fuel Cell Sci Technol, v. 3, n. 2. p. 8–11, 2006.

MAHATO, N. Progress in Material Selection for Solid Oxide Fuel Cell Technology: A Review. Progress in Materials Science, v. 72, p. 141–337, 2015.

MCLARTY, D.; BROUWER, J.; SAMUELSEN, S. Fuel cell–gas turbine hybrid system design part II: Dynamics and control. Journal of Power Sources, v. 254, p. 126–136, 2014.

NETO, Emilio Hoffman Gomes. Hidrogênio, evoluir sem poluir, a era do hidrogênio, das energias renováveis e das células de combustível. Curitiba: Brasil H2 Fuel Cell Energy, 2005.

SILVEIRA, J. L., MARTINS, E. L., GOMES, L.A..RAGONHA JR., L.F, Análise termodinâmica de sistemas de cogeração empregando células de combustível tipo carbonato fundido, Anais do XV Congresso Brasileiro de Engenharia Mecânica, Águas de Lindóia-SP, 1999.

TANNER, C. W., FUNG, K. Z., VIRKAR, A. V. The effect of porous composite electrode structure on solid oxide fuel cell performance: I - theoretical analysis. Journal of Electrochemical Society, Vol. 144, nº 1, pp. 21 - 30, 1997.

VAN WYLEN, G. J., SONNTAG, R. E. BORGNAKKE, C. Fundamentos da Termodinâmica Clássica. 6ª Ed. Edgard Blücher LTDA, São Paulo, 2003

VIRKAR, A. V., CHEN, J., TANNER, C.W., KIM, J.W. The role of electrode microstructure on activation and concentration polarizations in solid oxide fuel cells. Solid State Ionics. Vol. 131, pp. 189 - 198, 2000.

ZHU, L.; ZHANG, L.; VIRKAR, A. V. A parametric model for solid oxide fuel cells based on measurements made on cell materials and components. Journal of Power Sources, v. 291, p. 138–155, 2015.

7. RESPONSIBILITY NOTICE

The authors are the only responsible for the printed material included in this paper.